

# Ion Cyclotron Resonance

By T. H. Stix and R. W. Palladino \*

Calculations and experiments have been made on the ion cyclotron resonance phenomenon in a fully ionized gas. One is especially interested in this for directly heating the ions in a plasma. In ion cyclotron resonance (Fig. 1), an ion is in a magnetic field and a transverse electric field which oscillates at the ion cyclotron frequency. The ion velocity changes direction every half period, but so does the applied electric field and they remain in phase with each other. Energy is fed into the ion motion, and the ion will move in a growing spiral orbit.

If now we try to induce such a transverse electric field in a plasma, one asks whether some electron skin effect might prevent the penetration of the applied electric field into the plasma. However, the electrons are tied to the magnetic lines of force and they cannot carry a skin current. Thus, it turns out that if the plasma density is sufficiently low, an applied electric field will penetrate completely into the plasma and,

at resonance, each ion will move around a line of force in a tiny growing spiral orbit. In this manner, a low density plasma can be heated very effectively.

At higher densities, say  $10^{13}$  ions/cm<sup>3</sup>, this single particle picture is no longer valid. Ion currents induce an electric field inside the plasma which has a decelerating effect on the ions, and heating a moderately dense plasma at the ion cyclotron frequency

$$E \sim \cos \left[ \frac{e B_0}{mc} t \right]$$

360 1

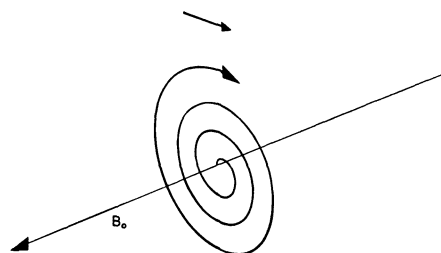


Figure 1. Acceleration of an ion at the ion cyclotron frequency

\* Project Matterhorn, Princeton University, Princeton, New Jersey.

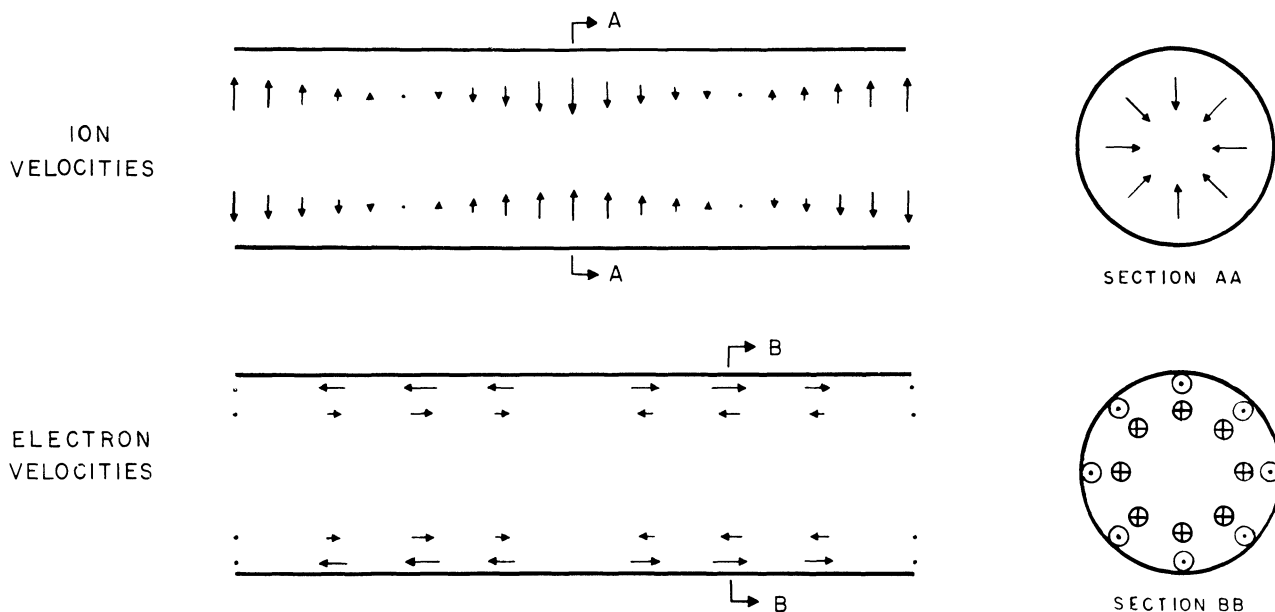
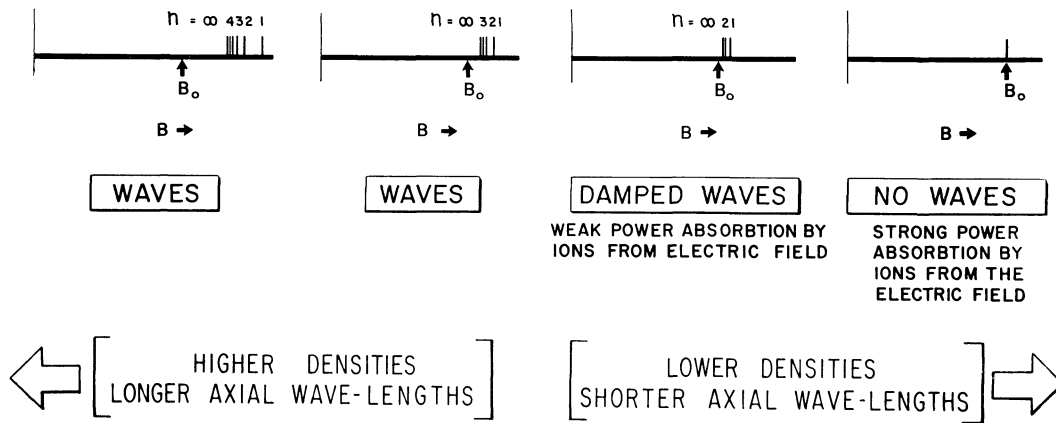


Figure 2. Ion cyclotron waves in a cylindrical plasma of uniform density surrounded by a vacuum in an axial magnetic field



$$2 \pi f = \frac{e B_0}{m c} \quad n = \text{radial mode number}$$

Figure 3. Spectra for ion cyclotron waves

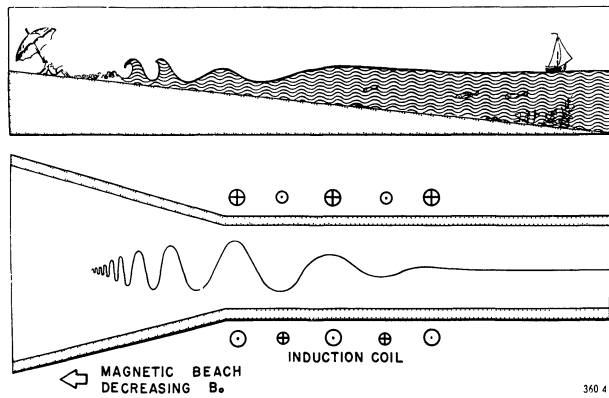


Figure 4. A "magnetic beach" for the thermalization of ion cyclotron waves

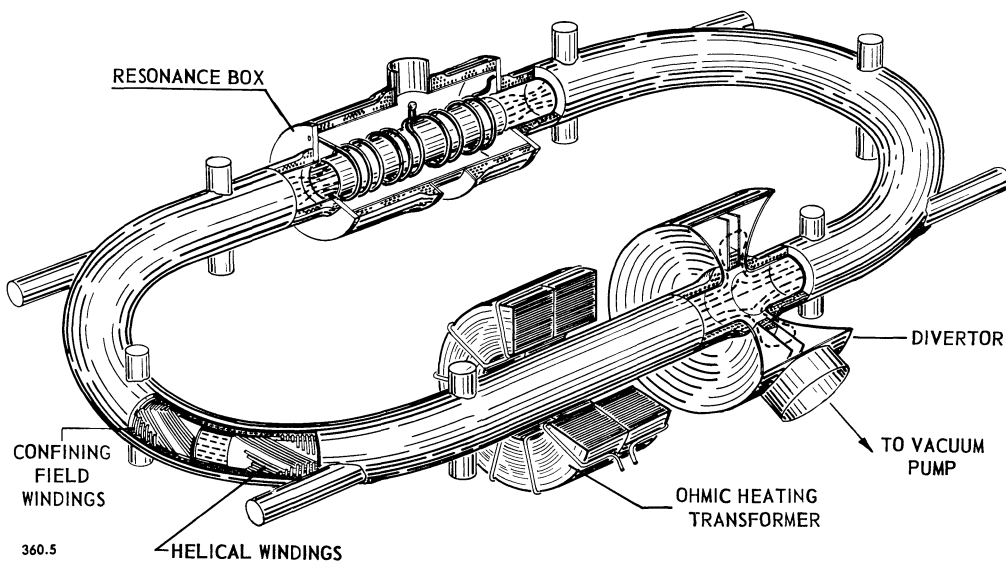


Figure 5. B-65 stellarator

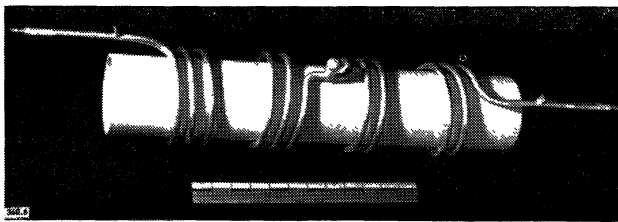


Figure 6. Induction coil

becomes very inefficient. However, if one keeps the frequency fixed, but goes to a slightly stronger magnetic field, one finds the existence of natural oscillations of the plasma. These natural oscillations, which we call "ion cyclotron waves", are in fact the short-wave, low-density limit for the extraordinary hydro-magnetic waves described by Alfvén and Åström. Figure 2 illustrates some of the standing wave patterns for these "ion cyclotron waves"; a side view and a cross section of a cylindrical plasma at the same instant of time are shown. The plasma is assumed to have a uniform density, to be surrounded by vacuum and to be in a strong axial magnetic field. Individual ions move in circles around the lines of force, but the phases and amplitudes of the ion velocities vary sinusoidally both in time and in space.

The ion flow has a non-zero divergence, which ordinarily would produce a large space charge and would result in large electric fields. However, since the ion flow pattern is periodic in the axial direction, the electrons are able to flow *along* the lines of force and neutralize the ion space charge. This axial flow of electrons is also illustrated in Fig. 2. Later on, in the

experimental work, we will find evidence that the flow of this neutralizing electron current along the lines of force heats the gas.

Figure 3 shows the spectra for ion cyclotron waves. The resonances are indicated as lines and are plotted against magnetic field strength. We look first at the picture denoted by "no waves". Here we have the lowest densities and, as a consequence, single particle acceleration of the ions in the electric field. The ions move in growing spiral orbits and there is strong power absorption by the ions from the electric field. There are no waves at this very low density condition.

For moderately high densities (see Fig. 3) there are ion cyclotron waves. The different lines indicate the different radial mode numbers and, for the high-density condition, all of the modes occur at magnetic fields considerably stronger than the cyclotron field,  $B_0$ . Once the ion cyclotron wave has been set up, the ions do not absorb energy from the electric fields. Therefore there is no damping of the wave.

The second picture in Fig. 3 shows the spectrum for ion cyclotron waves for somewhat lower densities. The various modes now occur at magnetic field values which are somewhat closer to the cyclotron field,  $B_0$ . There is still no damping of the waves. Now in the third picture, the density is quite low and the modes now occur at magnetic fields very close to the cyclotron field,  $B_0$ . This is an intermediate case between the ion cyclotron wave resonance and the single particle resonance. For this condition we have waves, but the ions begin to move in growing spiral orbits and pick up energy from the electric field. In this case we have ion cyclotron waves which are slightly damped.

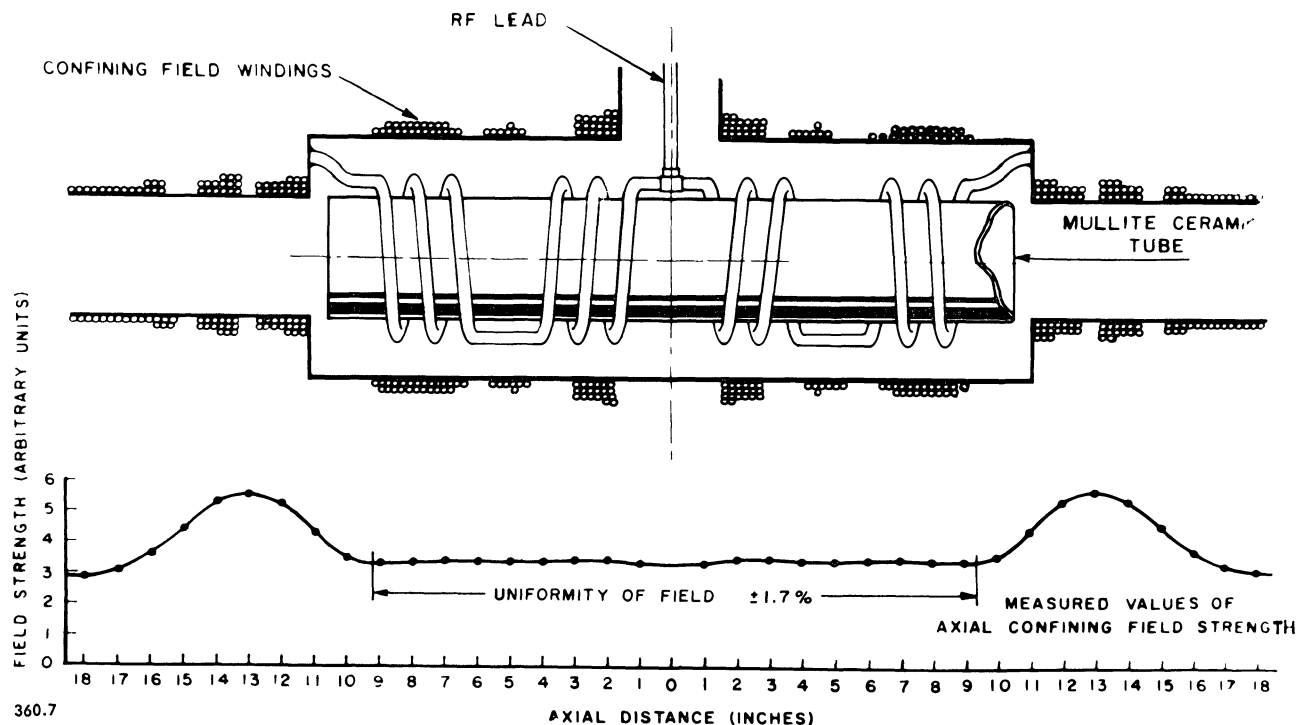


Figure 7. Resonance box, induction coil, field windings and confining field distribution

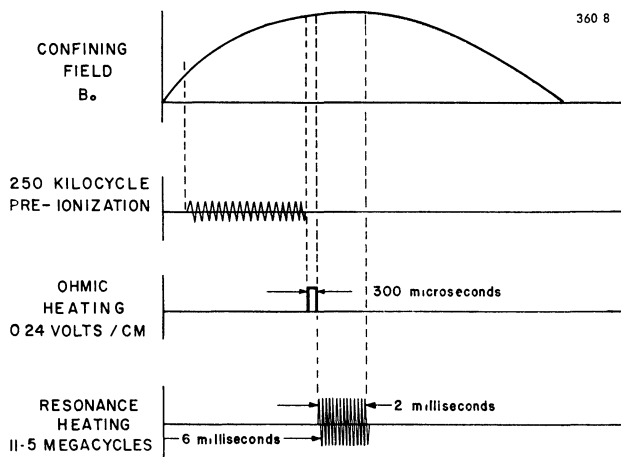


Figure 8. Time sequence for operation of the stellarator

The transition from the undamped waves to the slightly damped waves is particularly interesting because it provides a method for thermalizing the ion cyclotron waves; that is, for transforming the wave energy quickly into heat. It turns out that it is equally valid to talk about wavelengths instead of about densities, and it is the short wavelengths which are damped. To illustrate a plasma heating scheme, we make an analogy with ocean waves running up on a beach. A cross section of an ocean beach is shown in Fig. 4. The waves are moving in toward the shore and, because the water is getting shallower and shallower, the wavelength of the ocean waves becomes shorter and shorter. Finally, in the shallow water, the waves are unable to propagate and they "break"; the wave energy is transformed into heat. Similarly, one might use an induction coil to generate rather long wavelength ion cyclotron waves and allow these waves to propagate along the magnetic lines of force through a region where the magnetic field tapers off and becomes somewhat weaker. The wavelength becomes shorter and shorter and, finally, when the wavelength is sufficiently short the waves damp out and the wave energy goes into heating the ions. It would be in this magnetic "beach" region where the real heating of the gas would take place.

## EXPERIMENTAL

The ion cyclotron experiments were performed on the B-65 stellarator. A drawing of this machine is shown in Fig. 5. It is in the shape of a torus or race-track in which toroidal confining magnetic fields up to 20,000 gauss can be produced. It is equipped with a divertor and also with helical windings to give a rotational transform to the confining magnetic field. The large iron-core transformer is used to induce an ohmic heating current which flows along the magnetic lines of force. The resonance box on the far leg of the machine contains the induction coil for the resonance heating. A photograph of the induction coil is presented in Fig. 6. The coil is made up of four sections in which current flows in opposite directions

in adjacent sections of the coil. The coil is thus two wavelengths long and this establishes the wavelength of the ion cyclotron wave which we are trying to generate.

The resonance box is shown in more detail in Fig. 7. The induction coil surrounds a ceramic tube which is 53 cm long. The high voltage rf connection is brought into the center of the coil and the two ends of the coil are grounded. The windings for the confining magnetic field, which is uniform to within  $\pm 1.7\%$  over the length of the coil can be seen in Fig. 7. Also, at the bottom of Fig. 7 is a plot of the magnetic field intensity. Beyond each end of the coil there are magnetic mirror fields with a 3-2 mirror ratio. We have not yet installed the magnetic "beach" geometry on a stellarator.

The time sequence of the operations is depicted in Fig. 8. First the confining field rises and reaches a peak in about six milliseconds. While it is rising, an rf electric field directed along the magnetic lines of force breaks down the gas. Ohmic heating is turned on for a time just long enough to reach full ionization. The ohmic heating is then turned off and the resonance heating is turned on for two milliseconds (a diagram of the resonant heating circuit is shown in Fig. 9). The inductance of the coil is resonated with capacitors, and measurements are made of the input voltage and the input current. The phase angle between the input voltage and input current was obtained from Lissajous figures.

The plasma loading versus the strength of the confining magnetic field given in Fig. 10. The plasma loading graph is actually a plot of the input impedance to the parallel resonant circuit, but we have calibrated it in terms of the ratio,  $W$ , which is the rf power which goes into the plasma divided by the rf power which would be lost in the resistance of the induction coil if the induction coil had a  $Q$  of 300. The upper graph shows the plasma loading with an input power of about 300 watts. Although the working gas is deuterium, hydrogen comes into the discharge as an impurity and there is some loading in the vicinity of the hydrogen cyclotron field. The vertical line in Fig. 8 indicates the cyclotron field value for the hydrogen single particle resonance, obtained from an independent calibration of the magnetic field. At higher values of the confining magnetic field there appears strong plasma loading in the vicinity of the deuterium cyclotron resonance. Again, a vertical line indicates the value for the deuterium single particle resonance. Of particular interest is the asymmetry of the loading

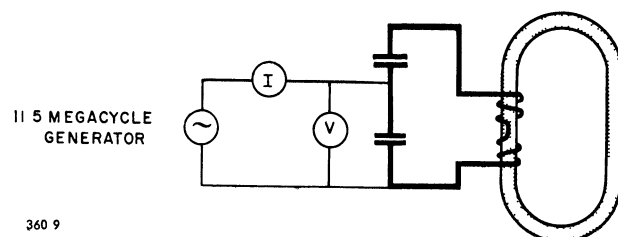
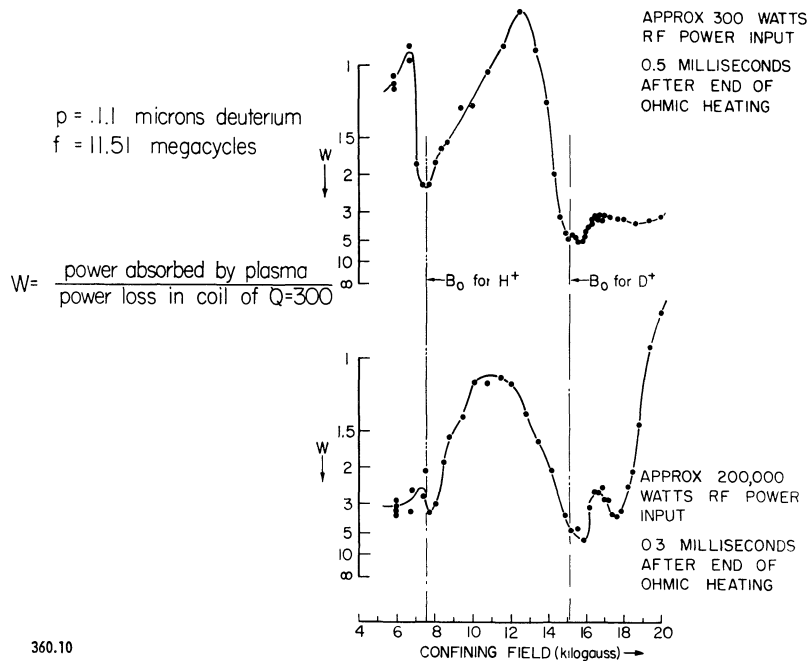


Figure 9. Diagram of resonant heating circuit



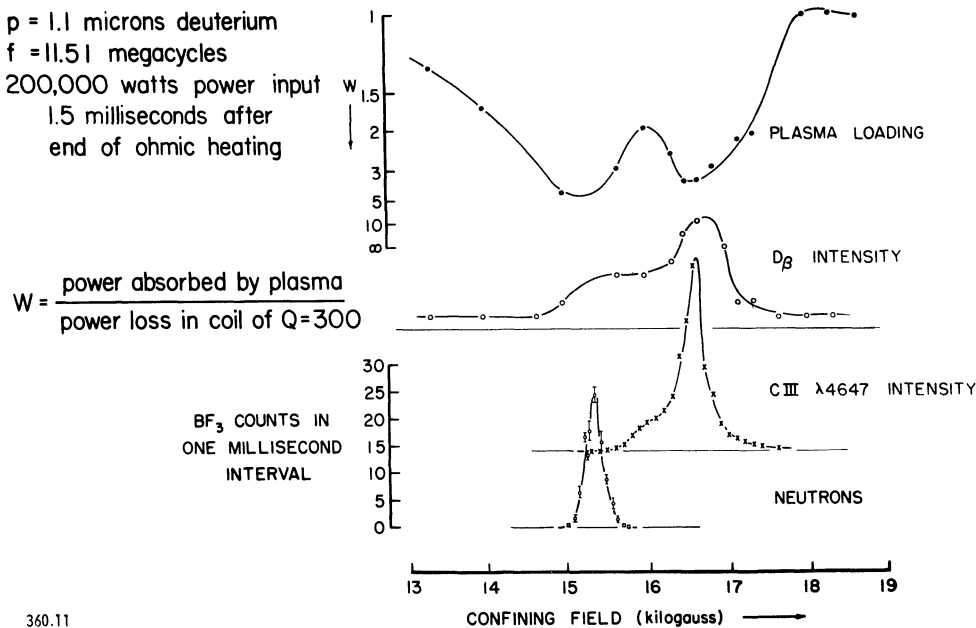
360.10

Figure 10. Plasma loading vs. confining field

curve, which shows greater loading at magnetic fields larger than the cyclotron field. At these larger values of the magnetic field one expects ion cyclotron waves to be generated, and the asymmetry in the loading indicates that power is going into this wave generation. The ratio  $W$  reaches a value of 5.5 at the peak of the resonance, which means that 5.5 times as much power is going into the gas as would go into an induction coil of  $Q$  equal to 300, or that the transfer efficiency from the induction coil to the gas is 85%.

The second loading curve is for an input power of roughly 200,000 watts. The high-power loading curve is remarkably similar to the lower power data, but now there is a clearer separation of the single particle resonance and of the wave generation resonance.

Some other effects which appear at the higher power level in the vicinity of the double peak are illustrated in Fig. 11. The top curve is the plasma loading in the vicinity of the double peak and is the same data as presented in Fig. 10, but is now plotted on an expanded



360.11

Figure 11. Plasma loading, spectral emission and neutron yield vs. confining field

scale. The second curve is the intensity of the Balmer beta,  $D\beta$ , spectral line of deuterium at 1.5 m sec after the end of ohmic heating phase. The neutral atoms which produce this light come back into the discharge from the wall of the stellarator tube. The third curve in Fig. 11 is the intensity of the CIII line  $\lambda 4647\text{\AA}$ . Both of these light intensity curves reach their peaks at the wave generation peak and indicate that the wave generation process is maintaining the electron density and the electron temperature at moderately high values. It seems probable that it is the electron neutralizing current (which flows along the lines of force as part of the ion cyclotron wave mechanism) which is keeping the electron temperature up through the processes of ohmic heating. The Doppler broadening of the CIII line indicates an ion temperature of about  $5 \times 10^6$  °K and it seems likely that the ions are in approximate thermal equilibrium with the electrons.

The bottom curve in Fig. 11 is the neutron counting rate measured with boron trifluoride counters. The observed neutron flux corresponds to  $10^4$  to  $10^5$  neu-

trons coming from the machine per pulse and the counting rate is very sharply peaked around the single particle deuterium resonance. It seems probable that these neutrons come from deuterons which were in the low density region outside the region of the main discharge column and which were accelerated to high velocities by the cyclotron resonance process.

Summarizing the experimental work, both the production of neutrons and the generation of ion cyclotron waves indicate that we are obtaining at least some penetration of the transverse electric fields into the plasma. Altogether, these rather preliminary data would seem to confirm the two extreme examples of behavior which are predicted by theory; namely, the low-density example where the single particle picture is valid and small numbers of particles may be accelerated to high velocities, and the high-density example where ion cyclotron waves are generated. The interesting intermediate case, where one generates ion cyclotron waves and then causes them to thermalize in a "magnetic beach" geometry, has not yet been investigated.